Supporting Information for

New Insight into GO, Cd(II), Phosphate Interaction and Its Role in GO Colloidal Behavior

Xuemei Ren[#†], Qunyan Wu[‼], Huan Xu[†], Dadong Shao[†], Xiaoli Tan[#†]*, Weiqun Shi[‼]*, Changlun Chen[†], Jiaxing Li[†], Zhifang Chai[‼§], Tasawar Hayat[‡ &], Xiangke Wang[#‡§]*

[#]School of Environment and Chemical Engineering, North China Electric Power University, Beijing 102206, P.R. China; [†]Institute of Plasma Physics, Chinese Academy of Sciences, P.O. Box 1126, 230031, Hefei, P.R. China; [‡]NAAM Research Group, Faculty of Science, King Abdulaziz University, Jeddah 21589, Saudi Arabia; [§]Collaborative Innovation Center of Radiation Medicine of Jiangsu Higher Education Institutions, P.R. China; [‼]Laboratory of Nuclear Energy Chemistry and Key Laboratory for Biomedical Effects of Nanomaterials and Nanosafety, Institute of High Energy Physics, Chinese Academy of Sciences, Beijing, 100049, China; [&] Department of Mathematics, Quaid−I−Azam University, Islamabad 44000, Pakistan

*: Corresponding author. Tel: +86−10−61772890; Fax: +86−10−61772890; Email: xkwang@ipp.ac.cn (X. Wang); tanxl@ipp.ac.cn (X. Tan); shiwq@ihep.ac.cn (W. Shi).

Environmental Science and Technology

Supplemental Information, 28 Pages, 19 Figures, and 1 Table.

Batch Experiments

The sorption of Cd(II) and/or P(V) on GO were studied using batch technique in a set of vials equipped with Teflon−lined screw caps. The desired concentrations of different components were obtained by adding the GO stock suspension and the stock solution of Cd(II), NaCl, and/or P(V) into the vials. Negligible volumes of 0.01 or 0.1 mol/L HCl or NaOH were added to the suspensions in each vial to achieve the desired initial pH values (2.0 – 12.0). After the vials involving these mixtures were put on a horizontal shaker and shaken at a constant speed of 120 rpm for 24 h, these vials were placed on a flat surface for 12 h without any disturbance to make sure of the complete settlement of the large sized GO aggregates. Finally, the residual concentrations of GO in the supernatant (mg/L) were measured by using UV−vis spectrophotometer (UV−2550, Perkin−Elmer) at a wavelength of 227 nm.[1] For the determination of unsorbed Cd(II)/P(V) concentrations in supernatant, the liquid and solid phases were separated by centrifugation at 15000 rpm for 20 min, and then the supernatants were filtered through 0.22 μm filtering membrane. The Cd(II) concentration in the supernatant was determined by the atomic absorption spectrophotometry. The phosphate concentration in the supernatant was determined by the blue phosphate−molybdate complex at the wavelength of 700 nm. The removal percentages of Cd(II) or P(V) on GO were calculated from the difference between the initial concentration (C_0, mmol/L) and the final one (C_e, mmol/L) (Removal percentage (%) = $(C_0-C_e)/C_0\times100\%$). All the experimental data were averages of

triplicate determinations, and the relative errors of the data were approximately 5%.

Theoretical Calculation.

For simplification, a graphene 5×4 supercell with the lattice constant of 2.46 Å modified by a hydroxyl group on the surface was employed as a computational model,[2, 3] shown in Figure S2. The dangling bonds of the graphene fragment were saturated by adding hydrogen atoms. To optimize the geometry, the quasi−relativistic small−core pseudo−potential ECP28MWB and associated ECP28MWB valence basis sets were adopted for cadmium,[4] while the 6−31G(d) basis set was applied for the other light atoms H, C, O and P. The neutral GO and deprotonated GO (dGO) were considered to simulate qualitatively low and high pH solution state, respectively. A hexa−coordinated $[Cd(H_2O)_6]^{2+}$ is the dominant species in aqueous, hence, the coordination number of Cd(II) cation are set to 6 for all initial optimized structures. Based on the different addition sequences in experiment, the structures of $[Cd(H_2O)_6]^{2+}$, $[Cd{-}P{-}5H_2O]^{+}$, $[GO{-}Cd{-}5H_2O]^{2+}$, and $[GO{-}Cd{-}P{-}4H_2O]^{+}$, and the corresponding deprotonated states were optimized at the B3LYP/6−31G(d) level of theory in the aqueous state. Their Gibbs free energies, including the thermal contribution, obtained at the same level were used to calculate the change of the Gibbs free energies of the reactions, which can indicate the relative binding ability of the GO with Cd(II).

Effect of Ionic Strength on Cd(II)/P(V) Removal

Evaluation of ionic strength effect on sorption behavior is an effective macroscopic method of inferring sorption mechanisms. To help compare and analyze the role of ionic strength variation, experiments are conducted to determine the sorption of Cd(II) on GO in 0.001 and 0.01 mol/L NaCl electrolyte solutions since the fact that Cl^- is the common ion in aqueous environment. One can see from Figure S3 that the removal percentage of Cd(II) on GO is not affected by ionic strength. It is well known that ion exchange or outer−sphere surface complexation is affected by ionic strength, whereas inner−sphere surface complexation is influenced by pH values.[5, 6] From the ionic strength independence, one can deduce that inner sphere complexation of Cd(II) with oxygen containing functional groups of GO is the main mechanism for Cd(II) removal by GO in the presence of P(V). Similarly, the P(V) removal is independent of ionic strength (Figure S14), suggesting surface complexation or strong chemical sorption is the dominate mechanism for P(V) removal by GO in the presence of Cd(II).

Size distributions of GO

The size distributions of the GO particles as a function of pH values in different systems have been monitored by a Zetasizer Nano–ZS90 Instrument (Malvern Co., U.K.) at 25 °C and presented in Figure S5. The responses of average sizes of GO in the 1 mmol/L NaCl solution and solution containing 1 mmol/L NaCl and phosphate (0.3 mmol/L P) to varying pH are contrary to those of residual concentrations of GO nanosheets in the supernatant (Figure 2A), with GO average sizes being quite constant

(~220 nm) from pH 4.0 to 12.0, then increasing sharply as pH decreases from 4.0 to 2.0. This increased average sizes (>1000 nm) below pH 4 are due to a reduction in the hydrophilicity of GO. The average sizes of GO in the presence of Cd(II) and Cd(II)+P(V) are very large in the pH range of 4.0 – 12.0. These is consistent with the results that the noticeable aggregations of GO in the presence of Cd(II) and Cd(II)+P(V) are observed in the whole tested pH ranges (Figure 2B in the manuscript). Figure S5 also shows that the average sizes of GO in solution containing Cd(II) and phosphate are larger than that of GO in solution only containing Cd(II), which is inconsistent with visual images of GO aggregate in solution only containing Cd(II) and in solution containing Cd(II) and phosphate (Figure 4B in the manuscript). We think the visual images of GO aggregate showed in Figure 4B are more credible. The larger GO aggregates are easier to sediment. The fast depositions of the large GO aggregate in the solution containing Cd(II) make them escape detection by particle size analyzer. Although particle size analyzer can provide the trend of GO size perturbations, it is not the accurate method to determine the actual GO sizes.

Effect of Initial Cd(II)/P(V) Concentration on P(V)/Cd(II) Removal

The batch experiments as a function of the Cd(II)/P(V) initial concentrations (Cd:P ratio) were conducted by taking different concentrations of Cd(II)/P(V) at a fixed initial pH (7.50 ± 0.05). The presence of Cd(II) can bridge negatively charged GO and P(V) anions, compress the double layer, neutralize negative charges of GO and P(V), and thus increase the affinity between P(V) and GO. Besides, Cd(II) can form

precipitate with P(V). In the presence of Cd(II), the retention percentage of P(V) (0.3 mmol/L P, pH 7.5) on GO increases from ~0% to ~40% as initial Cd(II) concentration increases from 0.07 to 0.25 mmol/L, and then maintains unchanged at Cd(II) concentration higher than 0.25 mmol/L (Figure S6). With the increase of initial Cd(II) concentration, more and more Cd(II) ions can form complexes with GO and provide more sorption sites for P(V), resulting in an increase of P(V) retention on GO through the formation of type A ternary surface complexes with Cd(II) as the bridge molecular. With the further increase of initial Cd(II) concentration, more Cd(II) ions can form precipitate with the limited P(V). This also leads to the increase of P(V) retention. However, the results of our addition sequences effect on the GO stability suggest that the formation of precipitate can stable GO. While, there is almost no GO in the supernatant in the presence of Cd(II) regardless of P(V) initial concentration. Therefore, the formation of Cd−P precipitate can be excluded. In contrast, the different initial concentrations of P(V) (0.03 – 0.3 mmol/L P) has no effect on Cd(II) (0.3 mmol/L, pH 7.5) retention on GO (Figure S7).The dependence of P(V) sorption on Cd(II) initial concentration and the independence of Cd(II) sorption on P(V) initial concentration further support the formation of type A ternary surface complexes, where Cd(II) bridges the GO surfaces and P(V) ions.

Sorption Isotherms of P(V) on GO

Figure S11 shows the sorption isotherms of P(V) on GO in the absence and presence of Cd(II) ($C_s = (C_0 - C_e)/m_{GO} \times V$, where C_s (mmol/g) was the concentration of P(V)

sorbed on GO, V (L) was the volume of the suspension, and m_{GO} (g) was the mass of the sorbents). One can see that in the absence of Cd(II), no P(V) ions were sorbed on GO at low P(V) concentrations. While the sorption of P(V) ions on GO increased with increasing P(V) concentration at high P(V) concentrations. This observed phenomenon may be attributed to P(V) form precipitates with the residual Mn^{2+} in GO suspension from GO preparation at high P(V) concentrations. The sorption isotherm of P(V) on GO in ternary system containing Cd(II) is higher than that of P(V) on GO in binary system without Cd(II). The positive effect of Cd(II) on P(V) sorption can be explained by Cd(II) complexation with oxygen containing functional groups of GO, reducing the electronegativity of GO and providing the sorptive sites for P(V), or by Cd(II) complexation with P(V), forming Cd−P aqueous complexes which have higher affinity to GO as compared with P(V), or by the formation of Cd−P precipitates. The first two suggests a surface−binding of P(V) through Cd(II) "bridge" between the GO surface and P(V). According to the Visual MINTEQ calculation (Figure S16), the $Cd_3(PO_4)_2$ become the thermodynamically favored phase with the increase of P(V) concentration. However, as mentioned above, there is almost no GO in the supernatant in the presence of Cd(II) regardless of initial P(V) concentration. Therefore, the formation of $Cd_3(PO_4)_2$ precipitate can be excluded. One can deduce that the enhanced sorption of P(V) by Cd(II) is mainly due to the formation of type A ternary surface complexes, and that the sorption of Cd(II) on GO occurs more quickly than its precipitation. The latter suggests that the presence of GO will hinder the

147 formation of $Cd_3(PO_4)_2$ precipitate.

148 **Sorption Isotherms of Cd(II) on GO**

149 The sorption of Cd(II) on GO as a function of Cd(II) concentration in the absence and
150 presence of P(V) was studied at pH 7.5 by varying Cd(II) concentration from 0.07 to
151 0.4 mmol/L, while keeping all other parameters constant. As shown in Figure S15, the
152 sorption of Cd(II) is found to decrease in the order of ternary (GO+Cd+P) system >
153 binary (GO+Cd) system. In both systems, the sorption capacity first increases rapidly
154 and then increases slowly with increasing Cd(II) equilibrium concentration, which
155 belongs to an L−type isotherm. At low initial Cd(II) solution concentration, the
156 surface area and the availability of sorption sites are relatively high, and the Cd(II)
157 ions are easily sorbed and removed. At higher Cd(II) initial solution concentration, the
158 total available sorption sites are limited, thus resulting in a slow increase in the
159 sorption capacity of GO. The sorption capacity in ternary (GO+Cd+P) system
160 increases much more rapidly than that in binary (GO+Cd) system, which may be
161 attributed to the formation of type A ternary surface complex or $Cd_3(PO_4)_2$ precipitate.
162 As shown in Figure S16, as the initial P(V) concentration is higher than 0.003 mmol/L
163 P, $Cd_3(PO_4)_2$ precipitate become thermodynamically favored phase for an aqueous
164 system containing 0.001 mol/L NaCl and 0.3 mmol/L Cd(II) in contact with an
165 atmosphere containing 0.00035 atm CO_2 at pH 7.5, based on MINTEQ calculation.
166 The Langmuir isotherm model was used in the present study to describe and
167 understand the sorption mechanism. The sorption experimental data of Cd(II) onto

GO in the absence of P(V) fit the Langmuir model well, while that of Cd(II) onto GO in the presence of P(V) cannot, indicating the sorption of Cd(II) onto GO in the presence of P(V) may not be monolayer formation on a homogeneous surface. This further support that the exposed P(V) in type A ternary surface complexes as a bridge between the sorbed Cd(II) and the dissolved one and/or the formation the Cd−P precipitate.

UV−vis Absorption Spectra of GO, Cd(II), P(V), GO with Cd(II), and GO with Cd(II) and P(V)

The UV−vis absorption spectra of GO, Cd(II), P(V), GO with Cd(II), and GO with Cd(II) and P(V) are shown in Figure S17. The Cd(II) and P(V) do not have a characteristic peak within the studied wavelength range (200 – 600 nm). GO has a characteristic peak at 227 nm. Meanwhile, the presence of Cd(II) and P(V) does not change the shape of GO's UV−vis absorption spectrum and characteristic peak. These results indicate that the presence of Cd(II) and P(V) does not affect the UV−vis measurement of GO.

Effect of Initial Cd(II) Concentration on GO Colloidal Behavior

The effect of initial Cd(II) concentration on GO colloidal behavior in the absence and presence of P(V) was studied at pH 7.5 by varying Cd(II) concentration from 0.067 to 0.4 mmol/L. Figure S18A shows that the increase of Cd(II) initial concentration decreases the GO concentration in solution. In the presence of P(V), the values of GO concentration decrease from 25 mg/L to ~ 2 mg/L as initial Cd(II) concentration

increases from 0.1 to 0.25 mmol/L, and then maintain unchanged at Cd(II) concentration higher than 0.25 mmol/L (Figure S18A). No matter whether the P(V) presents or not, Cd(II) can compress the electric double layer of GO, neutralize negative charges of GO, and coordinate with the oxygen containing groups of GO, resulting in destroying the stability of GO in solution. With the increase of initial Cd(II) concentration, more and more Cd(II) ions could interact with GO and make more GO aggregate, resulting in a decrease of the GO concentration in solution. At the low initial Cd(II) concentration of 0.15 mmol/L, the excess amounts of P(V) (0.3 mmol/L P) weaken the effectiveness of Cd(II) in destabilizing GO, so the value of GO concentration in the presence of P(V) is higher than that in the absence of P(V). At the initial Cd(II) concentration high than 0.15 mmol/L, the presence of P(V) has no notable effect on the colloidal behavior of GO in the Cd(II) aqueous solution.

Effect of Initial P(V) Concentration on GO Colloidal Behavior

The change in the GO concentration as a function of P(V) concentration in the absence and presence of Cd(II) was studied at pH 7.5 by varying P(V) concentration from 0.03 to 0.3 mmol/L P. Figure S18C showed both in the absence and presence of Cd(II), the initial P(V) concentration had no effect on the values of GO concentration. In the absence of Cd(II), the behaviors of the GO aggregation can be described as a balance between the anion (Cl^- and $H_2PO_4^-$) and cation (Na^+) interfacial concentrations. On one hand, the Na^+ concentrations increased from 1.03 to 1.3 mmol/L with increasing P(V) initial concentration, which is far below the critical

coagulation concentration values of GO (44 mmol/L NaCl reported by Chowdhury and coworkers[7] and 188 mmol/L NaCl reported by Wu and coworkers[8]). On the other hand, the presence of $H_2PO_4^-$ can weaken the effectiveness of Na^+ in destabilizing GO.[1] So, in the absence of Cd(II), GO is highly stable in the whole tested P(V) initial concentration.

In the presence of Cd(II), the values of GO concentration decreased notably. The supernatants in all vials became transparent. The great effect of Cd(II) on destabilizing GO was mainly due to the binding capacity with oxygen−containing groups of GO nanosheets by Cd^{2+}. The sorption isotherms of P(V) on GO in the presence of Cd(II) (Figure S13) show that the presence of Cd(II) has a positive effect on P(V) sorption due to the formation of type A ternary surface complexes at low P(V) concentrations and/or to the formation of $Cd_3(PO_4)_2$ precipitate at high P(V) concentrations. Based on the results of our addition sequences effect on the GO stability, the formation of precipitate can stable GO. However, there is almost no GO in the supernatant containing Cd(II) regardless of P(V) initial concentration (Figure S18D). Therefore, the formation of $Cd_3(PO_4)_2$ precipitate can be excluded. And the enhancement of P(V) removal and the reduction of GO stability in the presence of Cd(II) for ternary system is mainly attributed to the formation of the type A ternary surface complexes under our experimental conditions.

XPS Characterization and Analysis

In order to determine surface element composition, the XPS spectra were recorded

using a Thermo Escalab 250 electron spectrometer with an Al Kα radiation at 150 W. The XPS data were analyzed using the XPSPEAK software (version 4.1). The Gaussian−Lorentzian fitting were used following Shirley background subtraction.

The XPS spectra of survey and high resolution scans for the C 1s, O 1s, Cd 3d, and P 2p of GO before and after adsorption were shown in Figure S19. Deconvolution of the C 1s, O 1s, and Cd 3d spectra gives three peaks, three peaks, and two peaks, respectively. The peaks associated with oxygen functional groups in C 1s spectrum and the O 1s spectrum of GO without metal ions differs significantly from spectra for GO with adsorbed metal ions, both in the shape and the maximum position, providing the evidence that the oxygen−containing functional groups on the surface of GO take part in adsorption of metal ions. The slight differences (both in intensities and peak positions) can be observed for Cd 3d spectra without and with phosphate. Meanwhile, the occurrence of characteristic single peak of P 2p is observed in ternary system. Both suggest phosphate participate in Cd(II) adsorption in ternary system. Consideration the negatively charged GO and phosphate are electrostatically unfavorable, the formation of ternary surface complexes with Cd(II) as a bridge is the dominant mechanism.

According to XPS analysis, the element compositions of each sample are summarized in Table S1. The GO has a high content of O concentration (about 26%), indicating the existence of many potential adsorption sites. The P content of the (GO+Cd+P) sample is found to be 3.95%. The ratio of Cd to P for this sample is found to be about

1.4, which is lower than that in $Cd_3(PO_4)_2$ (1.5). Therefore, the $Cd_3(PO_4)_2$ precipitate is not formed under this condition, in accordance with the results of batch experiments and GO stability, which indicate that the removal of Cd(II) is not attributed to $Cd_3(PO_4)_2$ precipitation at pH < 9.5 when Cd(II), phosphate and GO are added simultaneously. The ratio of Cd to P in the (GO+Cd+P) sample is higher than 1, which further supports our deduce that the exposed P(V) in type A ternary surface complexes can act as the new sorptive sites to adsorb the dissolved Cd(II) in solution continuously via electrostatic attraction and complexation.

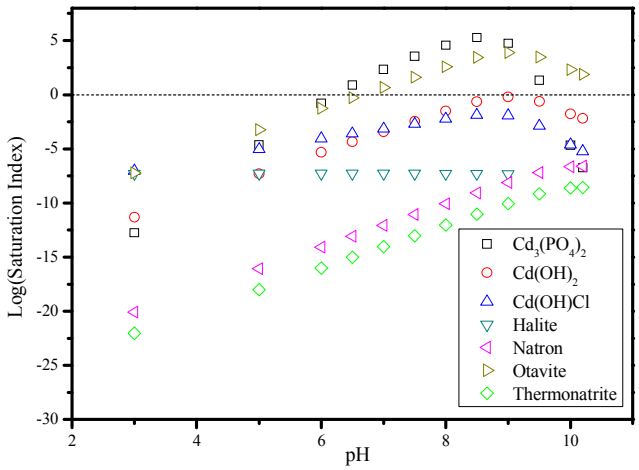

262

263 Figure S1. Saturation index of $Cd_3(PO_4)_2$, $Cd(OH)_2$, Cd(OH)Cl, halite, natron, otavite,

264 and thermonatrite calculated using Visual MINTEQ for an aqueous system containing

265 0.001 mol/L NaCl, 0.3 mmol/L Cd(II), and 0.3 mmol/L P(V) in contact with an

266 atmosphere containing 0.00035 atm CO_2.

267

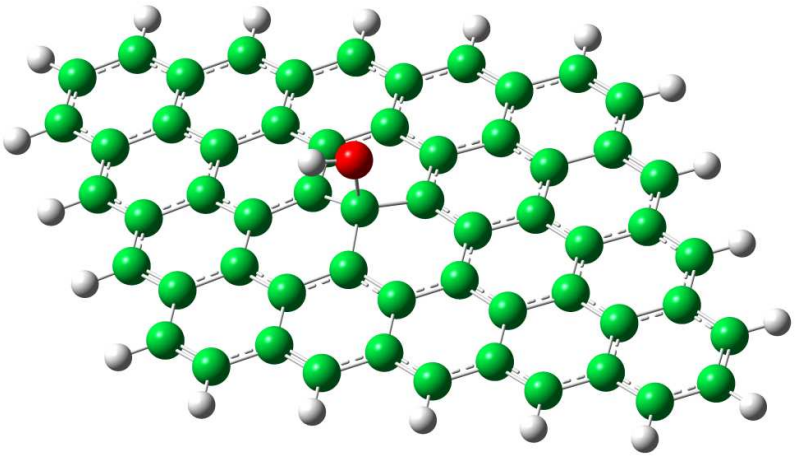

268

269 Figure S2. The graphene 5×4 supercell with lattice constant of 2.46 Å size modified

270 by a hydroxyl group on the surface for the computational model.

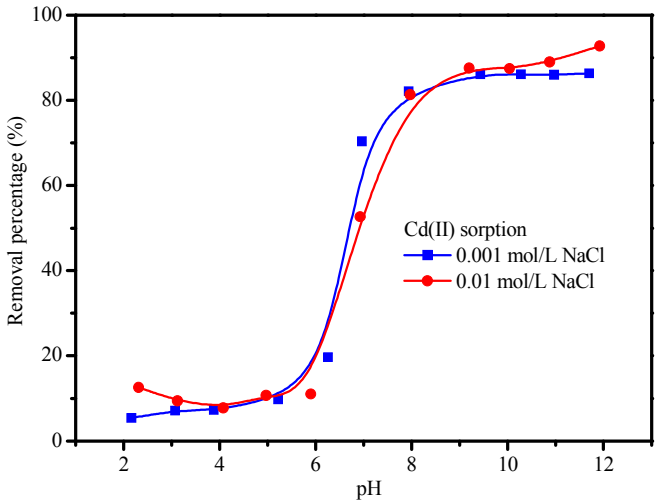

271

272 Figure S3 Effect of ionic strength on Cd(II) sorption on GO in the presence of P(V). T

273 =293 K, $C_{GO(initial)}$ = 25 mg/L, $C_{Cd(II)initial}$ = 0.3mmol/L, and $C_{P(V)initial}$ = 0.3mmol/L P.

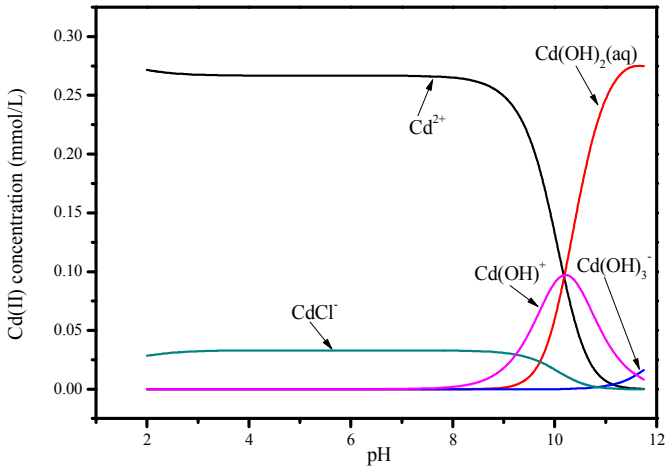

274

275 Figure S4 The concentrations of Cd(II) species at various pH values. $C_{[Cd(II)]initial}$ = 0.3

276 mmol/L. Cd(II) species were calculated by a chemical speciation model (Visual

277 MINTEQ version 3.0), which is downloaded freely from

278 http://www2.lwr.kth.se/English/OurSoftware/vminteq/download.html.

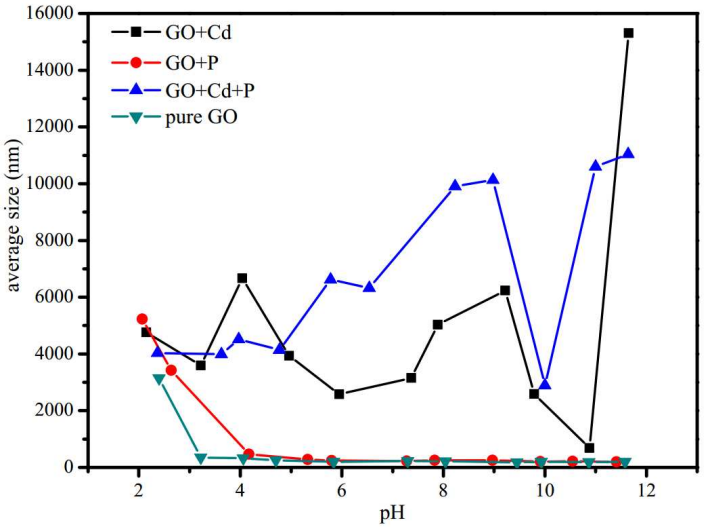

279

280 Figure S5 Size distribution of GO as a function of pH values in different systems.

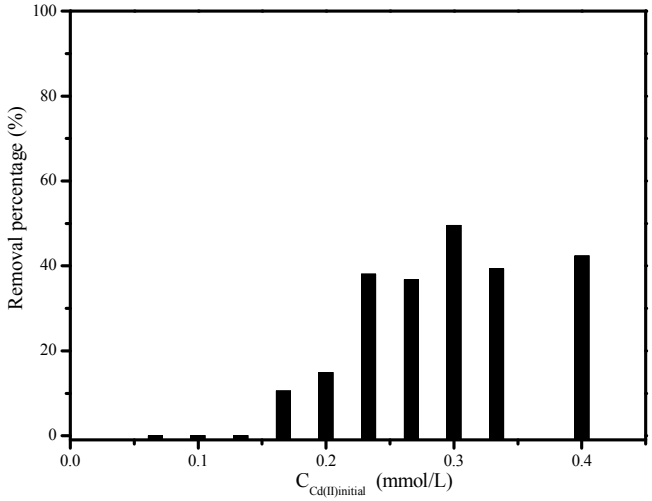

281

282 Figure S6 Effect of Cd(II) initial concentration on P(V) removal. pH = 7.5, $C_{P(V)initial}$ =

283 0.3 mmol/L P, $C_{GO(initial)}$ = 25 mg/L, and I = 0.001 mol/L NaCl.

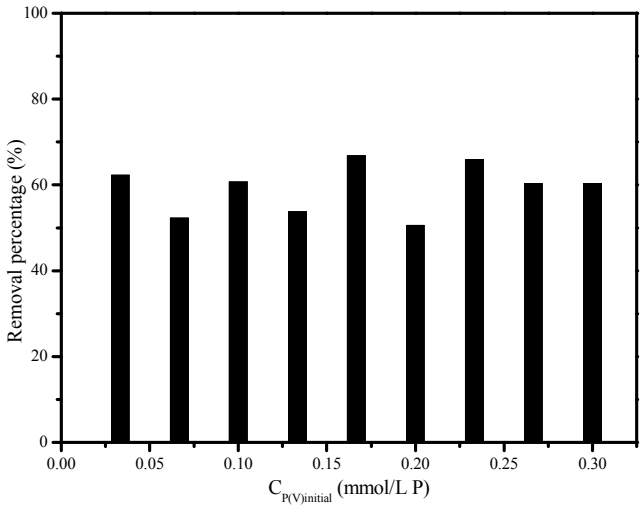

284

285 Figure S7 Effect of P(V) initial concentration on Cd(II) removal. pH = 7.5, $C_{Cd(II)initial}$

286 = 0.3 mmol/L, $C_{GO(initial)}$ = 25 mg/L, and I = 0.001 mol/L NaCl.

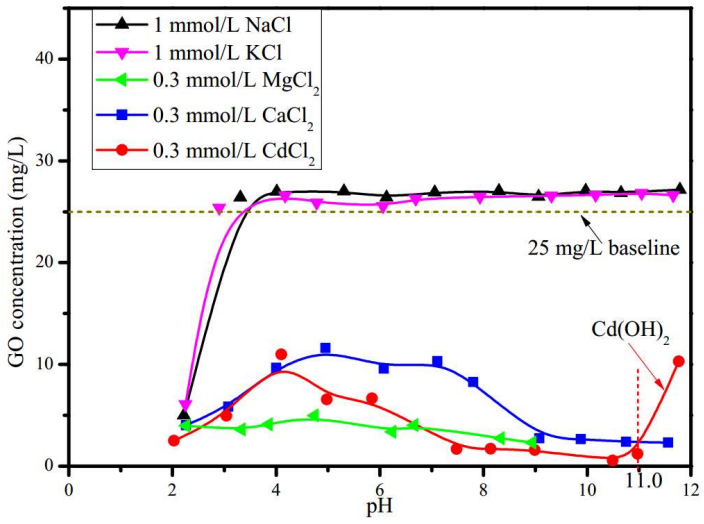

287

288 Figure S8 Residual concentrations of GO nanosheets in the supernatant as a function

289 of cation type.

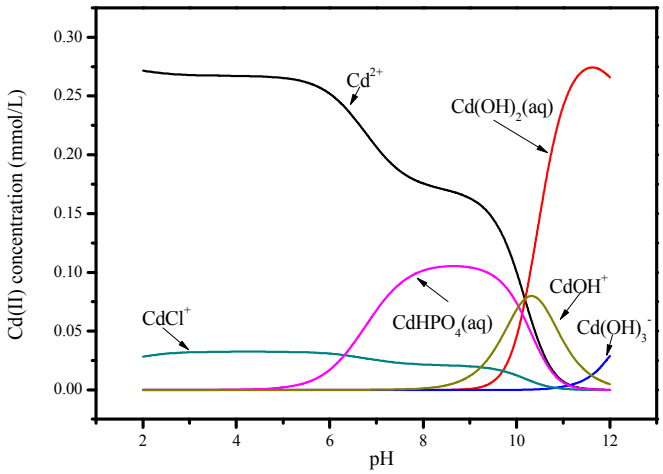

290

291 Figure S9 The concentrations of Cd(II) species in the presence of P(V) at various pH

292 values. $C_{[Cd(II)]initial}$ = 0.3mmol/L and $C_{[P(V)]initial}$ = 0.3mmol/L P. Cd(II) species in the

293 presence of P(V) were calculated by a chemical speciation model (Visual MINTEQ

294 version 3.0), which is downloaded freely from

295 http://www2.lwr.kth.se/English/OurSoftware/vminteq/download.html.

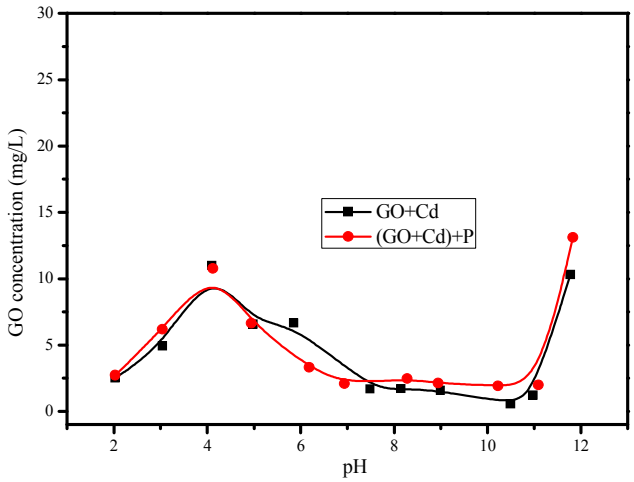

296

297 Figure S10 Effect of pH on the GO concentrations in GO+Cd and (GO+Cd)+P

298 systems. $C_{Cd(II)initial}$ = 0.3 mmol/L, $C_{P(V)initial}$= 0.3 mmol/L P, $C_{GO(initial)}$ = 25 mg/L, and

299 I = 0.001 mol/L NaCl.

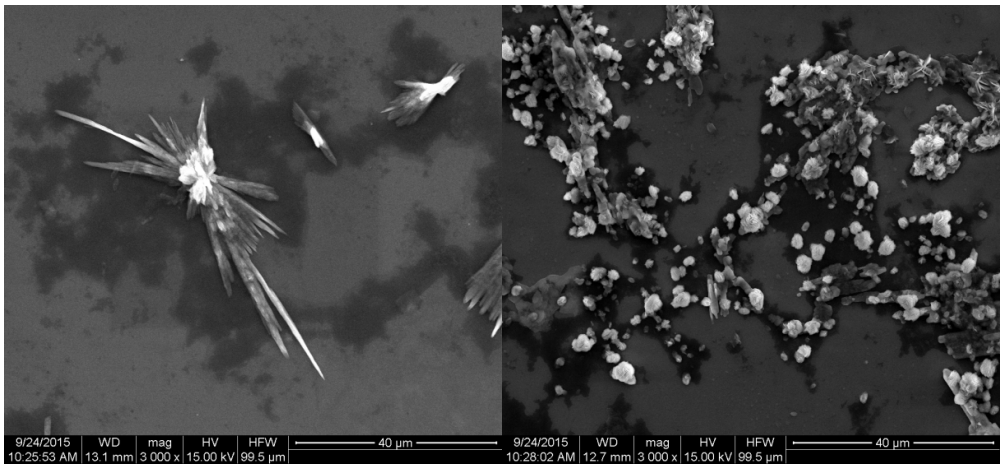

300

301 Figure S11 SEM images of GO aggregates in the Cd(II) (the left one) and Cd(II)+P(V)

302 (the right one) aqueous solutions.

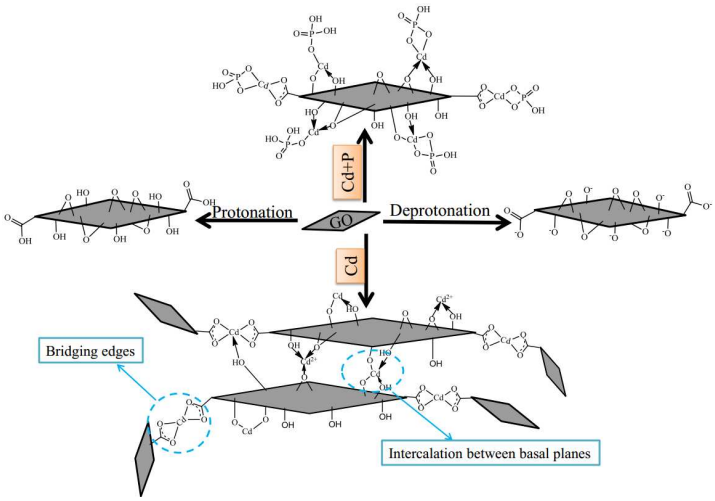

303

304 Figure S12 Interaction mechanisms of pH, Cd(II), and P(V) with GO.

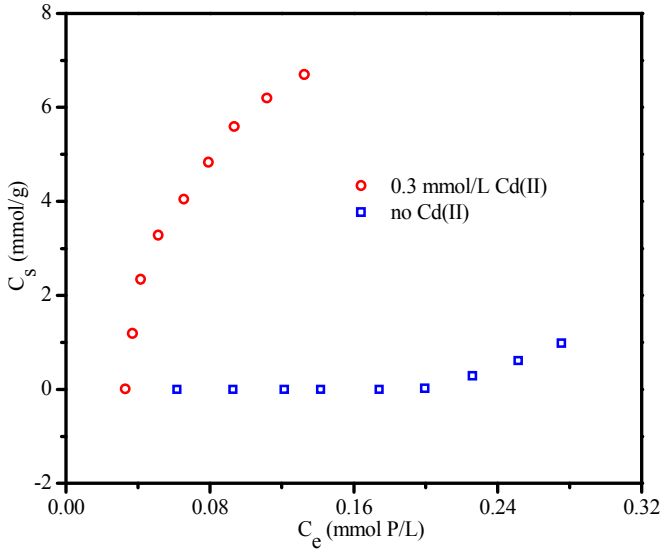

305

306 Figure S13 Sorption isotherms of P(V) on GO in the absence and presence of Cd(II).

307 pH = 7.5, $C_{Cd(II)initial}$ = 0.3 mmol/L, $C_{GO(initial)}$ = 25 mg/L, and I = 0.001 mol/L NaCl.

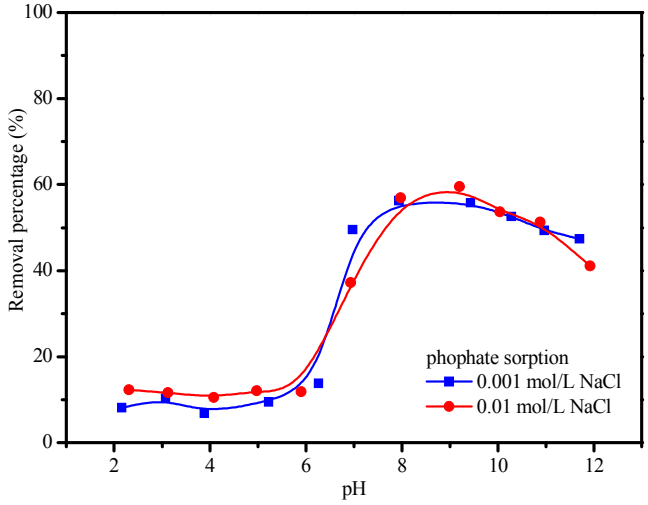

308

309 Figure S14 Effect of ionic strength on P(V) sorption on GO in the presence of Cd(II).

310 $C_{GO(initial)}$ = 25 mg/L, $C_{Cd(II)initial}$ = 0.3 mmol/L, and $C_{P(V)initial}$ = 0.3 mmol/L P.

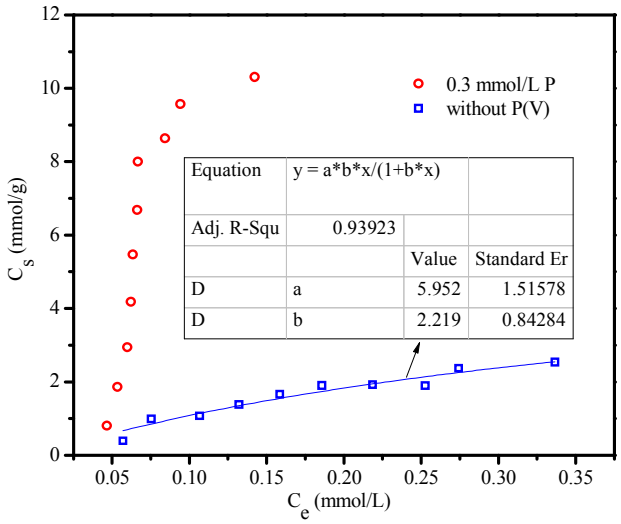

311

312 Figure S15 Sorption isotherms of Cd(II) on GO in the absence and presence of P(V).

313 pH = 7.5, $C_{P(V)initial}$ = 0.3 mmol/L P, $C_{GO(initial)}$ = 25 mg/L, and I = 0.001 mol/L NaCl.

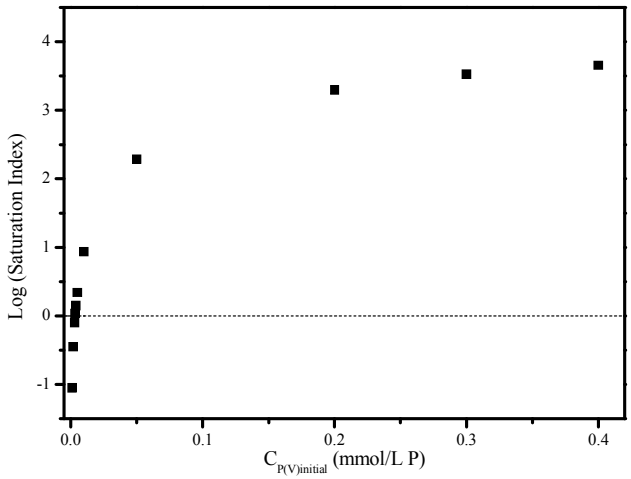

314

315 Figure S16 Saturation index of $Cd_3(PO_4)_2$ as a function of initial P(V) concentration

316 calculated using Visual MINTEQ for an aqueous system containing 0.001 mol/L NaCl

317 and 0.3 mmol/L Cd(II) in contact with an atmosphere containing 0.00035 atm CO_2 at

318 pH 7.5.

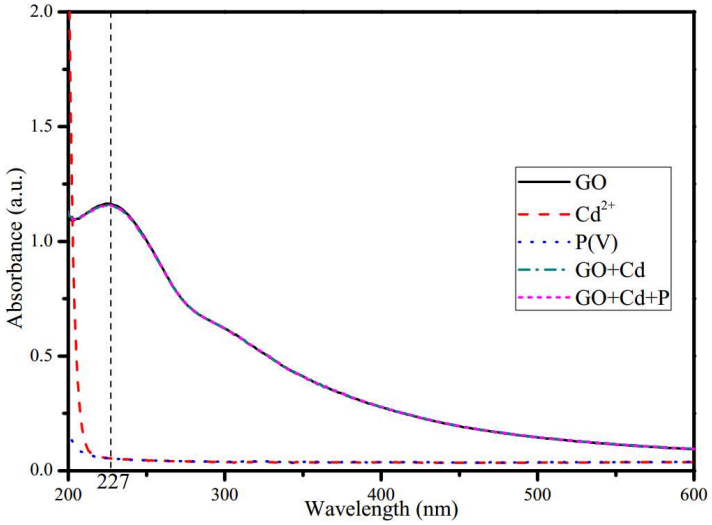

Figure S17 UV−vis absorption spectra of GO, Cd(II), P(V), GO with Cd(II), and GO with Cd(II) and P(V).

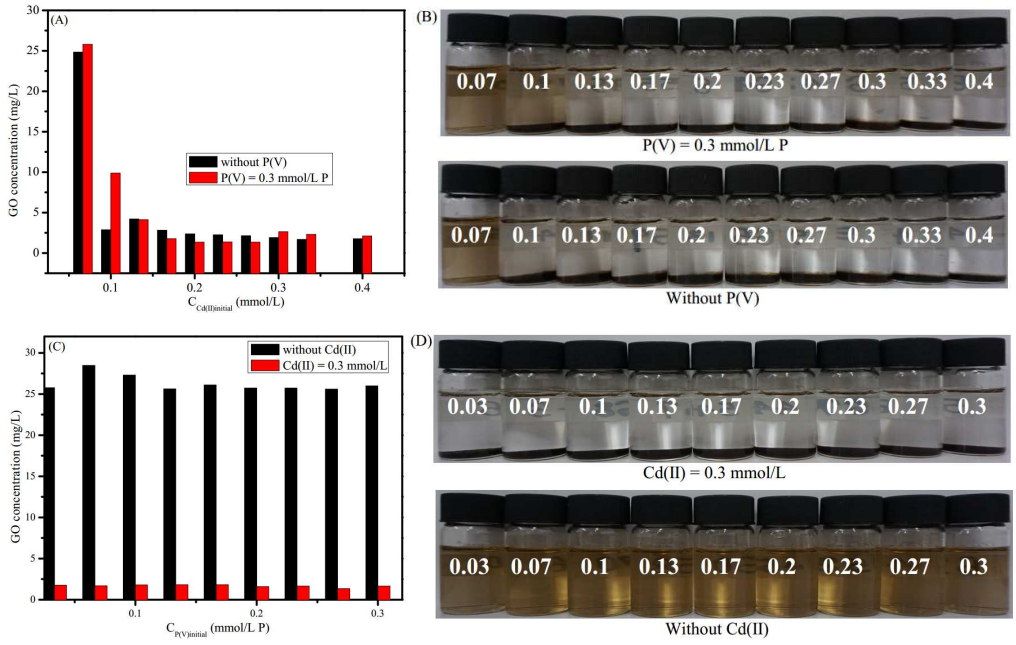

Figure S18 (A) Residual concentrations of GO nanosheets in the supernatant as a function of the Cd(II) initial concentration in the absence and presence of P(V); (B) Optical photograph showing the dispersion of GO as a function of the Cd(II) initial concentration in the absence and presence of P(V). pH = 7.5, $C_{GO(initial)}$ = 25 mg/L, $C_{P(V)initial}$ = 0.3 mmol/L P, and I = 0.001 mol/L NaCl. (C) Residual concentrations of

GO nanosheets in the supernatant as a function of the P(V) initial concentration in the absence and presence of Cd(II); (D) Optical photograph showing the dispersion of GO as a function of the P(V) initial concentration in the absence and presence of Cd(II). pH = 7.5, $C_{GO(initial)}$ = 25 mg/L, $C_{Cd(II)initial}$ = 0.3 mmol/L, and I = 0.001 mol/L NaCl.

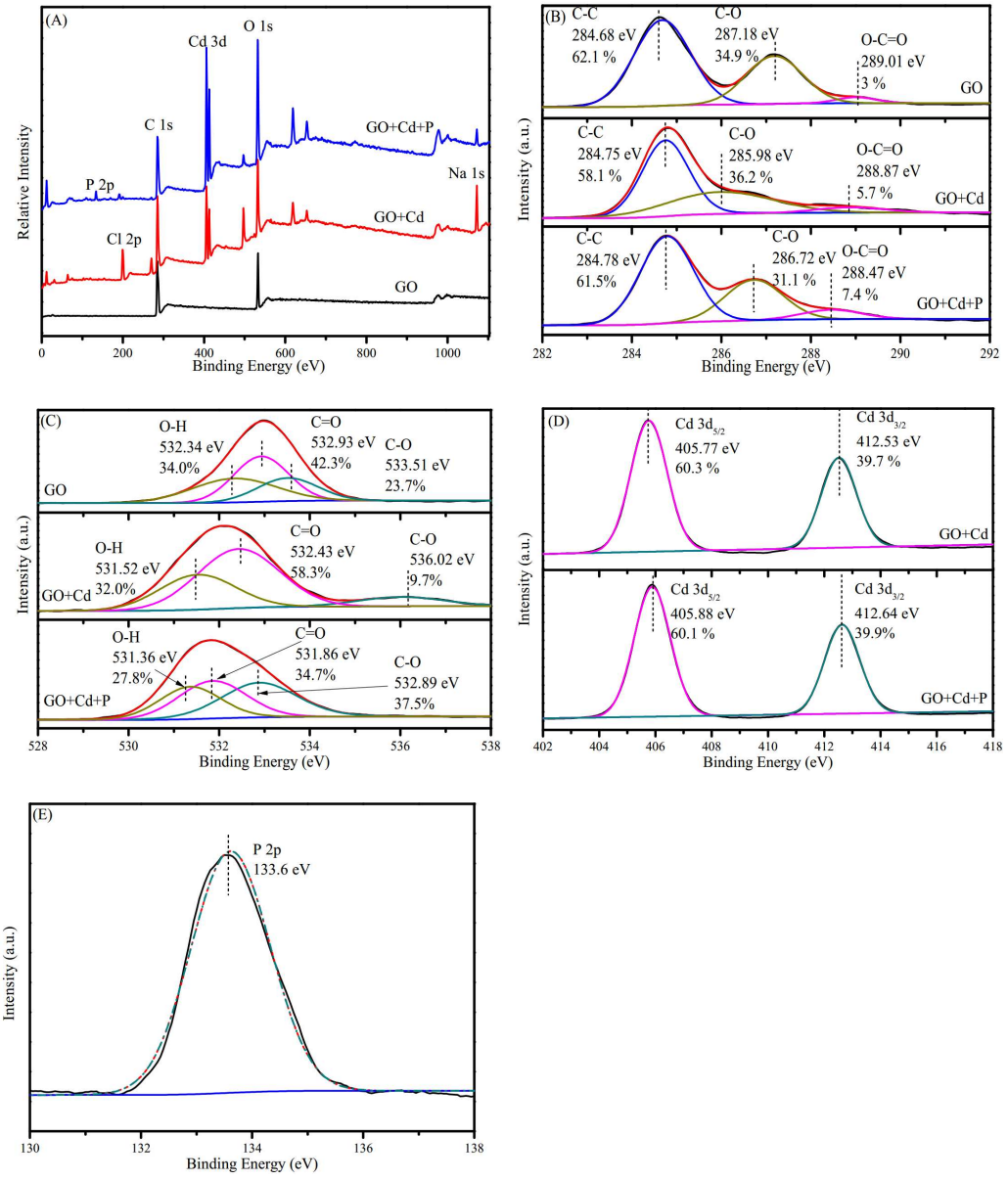

Figure S19 XPS survey scan and high resolution scans of GO, GO+Cd, and GO+Cd+P. (A) Total survey scans, (B) C 1s peaks, (C) O 1s peaks, (D) Cd 3d peaks,

(E) P 2p peak. C_{GO} = 25 mg/L, pH = 7.5, I = 0.001 mol/L NaCl.

Table S1 Elemental compositions of GO before and after Cd(II) and phosphate adsorption as determined through XPS

Sample	Element composition					
	C(%)	O(%)	Cd(%)	P(%)	Na(%)	Cl(%)
GO	74.21	25.79	0	0	0	0
GO+Cd	60.96	22.18	2.99	0	5.98	7.89
GO+Cd+P	54.46	33.41	5.61	3.95	1.86	0.7

346 REFERENCES

347 (1) Ren, X. M.; Li, J. X.; Tan, X. L.; Shi, W. Q.; Chen, C. L.; Shao, D. D.; Wen, T.;
348 Wang, L. F.; Zhao, G. X.; Sheng, G. P.; Wang, X. K. Impact of Al_2O_3 on the
349 aggregation and deposition of graphene oxide. *Environ. Sci. Technol.* **2014,** *48*(10),
350 5493-5500.

351 (2) Wu, Q. Y.; Lan, J. H.; Wang, C. Z.; Zhao, Y. L.; Chai, Z. F.; Shi, W. Q.
352 Understanding the interactions of neptunium and plutonium ions with graphene oxide:
353 Scalar-relativistic DFT investigations. *J. Phys. Chem. A* **2014,** *118*(44), 10273-10280.

354 (3) Wu, Q. Y.; Lan, J. H.; Wang, C. Z.; Xiao, C. L.; Zhao, Y. L.; Wei, Y. Z.; Chai, Z.
355 F.; Shi, W. Q. Understanding the bonding nature of uranyl ion and functionalized
356 graphene: A theoretical study. *J. Phys. Chem. A* **2014,** *118*(11), 2149-2158.

357 (4) Martin, J. M. L.; Sundermann, A. Correlation consistent valence basis sets for use
358 with the Stuttgart-Dresden-Bonn relativistic effective core potentials: The atoms
359 Ga-Kr and In-Xe. *J. Chem. Phys.* **2001,** *114*(8), 3408-3420.

360 (5) Yang, S. T.; Sheng, G. D.; Tan, X. L.; Hu, J.; Du, J. Z.; Montavon, G.; Wang, X.
361 K. Determination of Ni(II) uptake mechanisms on mordenite surfaces: A combined
362 macroscopic and microscopic approach. *Geochim. Cosmochim. Acta* **2011,** *75*(21),
363 6520-6534.

364 (6) Tan, X. L.; Wang, X. K.; Geckeis, H.; Rabung, T. Sorption of Eu(III) on humic
365 acid or fulvic acid bound to hydrous alumina studied by SEM-EDS, XPS, TRLFS,
366 and batch techniques. *Environ. Sci. Technol.* **2008,** *42*(17), 6532-6537.

(7) Chowdhury, I.; Duch, M. C.; Manuskhani, N. D.; Hersam, M. C.; Bouchard, D. Colloidal properties and stability of graphene oxide nanomaterials in the aquatic environment. *Environ. Sci. Technol.* **2013,** *47*(12), 6288-6296.

(8) Wu, L.; Liu, L.; Gao, B.; Muñoz-Carpena, R.; Zhang, M.; Chen, H.; Zhou, Z.; Wang, H. Aggregation kinetics of graphene oxides in aqueous solutions: Experiments, mechanisms, and modeling. *Langmuir* **2013,** *29*(49), 15174-15181.